

# Efficient and Effective Dropout for Deep Convolutional Neural Networks

Shaofeng Cai, Yao Shu, Gang Chen, *Member, IEEE*,  
Beng Chin Ooi, *Fellow, IEEE*, Wei Wang, Meihui Zhang *Member, IEEE*



**Abstract**—Convolutional Neural networks (CNNs) based applications have become ubiquitous, where proper regularization is greatly needed. To prevent large neural network models from overfitting, dropout has been widely used as an efficient regularization technique in practice. However, many recent works show that the standard dropout is ineffective or even detrimental to the training of CNNs. In this paper, we revisit this issue and examine various dropout variants in an attempt to improve existing dropout-based regularization techniques for CNNs. We attribute the failure of standard dropout to the conflict between the stochasticity of dropout and its following Batch Normalization (BN), and propose to reduce the conflict by placing dropout operations right before the convolutional operation instead of BN, or totally address this issue by replacing BN with Group Normalization (GN). We further introduce a structurally more suited dropout variant Drop-Conv2d, which provides more efficient and effective regularization for deep CNNs. These dropout variants can be readily integrated into the building blocks of CNNs and implemented in existing deep learning platforms. Extensive experiments on benchmark datasets including CIFAR, SVHN and ImageNet are conducted to compare the existing building blocks and the proposed ones with dropout training. Results show that our building blocks improve over state-of-the-art CNNs significantly, which can be ascribed to the better regularization and implicit model ensemble effect.

**Index Terms**—Convolutional Neural Networks, Dropout, Drop-Conv2d, Regularization, Variance Shift, Convolutional Building Blocks

## 1 INTRODUCTION

Deep neural networks (DNNs) have achieved remarkable success in a variety of fields including computer vision [19], [7], [13], natural language processing and healthcare analytics [3], [39]. To increase model capacity for better performance, DNNs become larger and deeper with typically hundreds of layers and millions of parameters [7], [14], [35]. However, large DNN models are prone to overfitting, and therefore proper regularization is greatly needed for the training of DNNs.

To improve generalization performance, many explicit and implicit regularization techniques are proposed, such as early stopping, weight decay, data augmentation [4] and

etc. Dropout [10], [27] is arguably the most prominent regularization technique used in practice, due to its efficiency and effectiveness. Specifically, for each training iteration, the standard dropout randomly samples a set of neurons and deactivates them, and then the training is conducted on the resultant subnet, which incurs negligible computational overhead. Thereby, a new subnet is sampled and trained for each iteration. The full network can thus be considered as an ensemble of an exponentially large number of subnets whose parameters are shared. Besides the model ensemble effect, dropout also regularizes the networks by discouraging co-adaptation [27] between neurons and therefore contributes to more robust feature extraction.

However, recent attempts to apply dropout to convolutional neural networks [7], [37], [14] (CNNs) fail to obtain noticeable performance improvement. Initially, dropout [27], [10] is introduced to fully connected layers [19], which are however replaced by a global average pooling layer [22] thereafter. Many attempts have also been made to apply dropout to convolution layers. For instance, WRN [37] applies a dropout layer between two wide convolution layers of the residual block and reports improved accuracy. However, dropout for these CNNs is still adopted at the neuron level, which turns out to be less effective. Even detrimental effects are observed [8] when introducing dropout to the identity mapping of the residual block in ResNet [7]. The effectiveness of dropout for CNNs is further reduced by the introduction of other regularization techniques such as data augmentation and batch normalization [16] in particular.

At a high level, the effectiveness of dropout training can be largely attributed to the regularization and ensemble effect engendered by random subnet sampling for training. Following the same methodology, various dropout variants are also proposed injecting randomness into different CNN structural components, such as input patches [4], connections [33], neurons [27], activation maps [30], [6], transformation paths [20], [35], residual blocks [15], [36]. Although many of these variants can improve over the standard dropout to some extent, a closer and comprehensive investigation is much needed to provide consistently efficient and effective dropout training for CNNs.

To better integrate dropout into CNNs, we revisit the existing dropout variants applied to different structural components, notably neurons, channels and paths. In this paper,

- S. Cai, Y. Shu, B.C. Ooi, W. Wang are with National University of Singapore, Singapore 117417. E-mail: [shaofeng, shuyao95, ooibc, wangwei]@comp.nus.edu.sg
- G. Chen is with Zhejiang University, Hangzhou 310027, China. E-mail: cg@cs.zju.edu.cn
- M. Zhang is with Beijing Institute of Technology, Beijing, China 100081. Email: meihui\_zhang@bit.edu.cn

we present a unified framework to formulate and examine the three primary dropout variants, which are denoted as Drop-Neuron, Drop-Channel and Drop-Path respectively. To uncover the reason behind the ineffectiveness of existing dropout methods for convolutional layers, we investigate the interaction between dropout and other common techniques adopted in CNNs, i.e., data augmentation and batch normalization [16] (BN) in particular. We find that drop-channel is generally more effective in improving CNN training than drop-neuron. We also note that for the neuron and channel level dropout, namely drop-neuron [21] and drop-channel, their conventional usage is in conflict with BN, which is adopted widely in CNNs to stabilize the first two moments (i.e., mean and variance) of its output distribution, whereas the random deactivation of the basic components (i.e., neurons and channels respectively) with the drop-neuron and drop-channel training disrupts such stability. We then propose improved convolutional building blocks with drop-neuron/drop-channel and common CNN layers, including dropout, convolution, batch normalization layer for ease of use (see Figure 3). We further examine various drop-path variants, i.e., dropout applied at the path level where transformation branches are randomly dropped during training [20], [35], [15], [36], and find that path-dropping is largely effective in improving generalization. Based on these observations, we integrate drop-channel and drop-path and propose a more efficient and effective dropout variant Drop-Conv2d. For convolutional layers trained with drop-conv2d, each transformation branch between input and output channels is replicated  $P$  times for larger model capacity, and these branches are randomly dropped during training to harness the dropout training benefits. Then during inference, these branches can be readily merged back into one branch with no additional cost.

The advantages of the proposed building blocks are threefold. Firstly, these dropout variants can be readily implemented as CNN building blocks in existing deep learning platforms such as Pytorch, TensorFlow or Apache SINGA<sup>1</sup> initiated by us to support various DL-based applications, as illustrated in Figure 1. Second, all these dropout variants are computationally lightweight and incur negligible computational overhead. Third, the adoption of different dropout variants in convolutional layers of CNNs, especially drop-conv2d, provides a more effective regularization. To support these claims, extensive experiments are conducted over state-of-the-art CNNs. We adopt widely benchmarked datasets CIFAR-10, CIFAR-100, SVHN and ImageNet, where significant accuracy improvement is observed even upon batch normalization and extensive data augmentation. The main contributions can be summarized as follows:

- We present a unified framework for analyzing dropout variants in CNNs. Specifically, we investigate the failure of drop-neuron and drop-channel, which is mainly due to their conflict with BN in the convolutional block.
- We propose convolutional building blocks and drop-conv2d, which are better in line with the dropout training mechanism and are readily applicable to existing CNN architectures.

1. <https://singa.apache.org/>

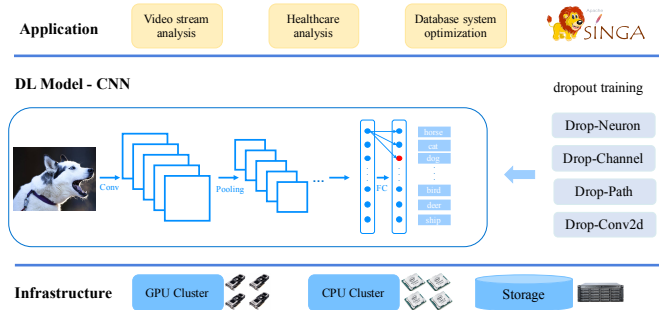


Fig. 1: Supporting complex analytics with dropout training.

- We conduct extensive experiments to examine different dropout variants and confirm the effectiveness of our proposed building blocks, and consistently achieve significant improvement for CNNs.

The remainder of the paper is organized as follows. Section 2 introduces the background. In Section 3, we formulate the convolutional transformation in a unified framework, based on which training mechanisms of dropouts are examined, and improved building blocks and drop-conv2d are proposed for deep CNNs. Experimental evaluations of our proposed building blocks are provided in Section 4. We conclude this paper in Section 5.

## 2 BACKGROUND

### 2.1 Deep Convolutional Neural Networks

One notable trend of recent convolutional neural networks (CNNs) is their growing depth and width. AlexNet [19] develops an 8 layer CNN for the large image classification dataset ImageNet and achieves great success. The subsequent VGG [26] and GoogLeNet [29] push the depth of CNNs to 19 and 22 respectively by stacking their respective basic convolutional building blocks, e.g., Inception module in GoogLeNet. ResNet [7] further proposes the residual connection that enables the training of ever deep CNNs over 1000 layers. However, pushing CNN architectures deeper alone does not bring further benefits [7], [31], and many CNN architectures instead grow wider [37], for larger model capacity and the ease of training. [22] replaces the filter kernel of the convolution with a multilayer perceptron, which facilitates interactions between input channels. CNNs such as Inception series [29] and ResNeXt [35] instead utilize group convolution [19], proposing the multi-branch convolution. Other CNN building blocks of different connection topology and transformations are also proposed, such as Inception modules [29], residual blocks [7], [8], dense connection blocks [14] and remarkably various Neural Architecture Search blocks [40], [23], [25] in recent years.

### 2.2 Dropout for Deep Neural Networks

Regularization is essential for deep neural networks, and many regularization methods have been proposed, such as weight decay, data augmentation, batch normalization [16] and etc. Dropout [27], [10] is arguably the most prominent regularization technique used in practice. [32] shows that dropout performs a form of adaptive regularization for

generalized linear models, which is first-order equivalent to an  $L_2$  regularizer. Further, dropout provides immediately the magnitude of the regularization, which is adaptively scaled by the inputs and the variance of the dropout variables [1], [5], [17] analyze dropout in the Bayesian inference framework for uncertainty modeling.

Many relevant implicit model ensemble techniques based on dropout are also proposed. Swapout generalizes dropout with a stochastic training method, which samples subnet for training from either dropout, stochastic depth [15] or the residual connection [7]. DropConnect [33] instead introduces randomness to connections and randomly deactivates connections during training. Model Slicing [2] randomly trains sliced subnets during training so that runtime accuracy-efficiency trade-offs can be achieved with these subnets. More dropout variants are also proposed injecting randomness into different structural components. SpatialDropout [30] shows that adding one additional layer with dropout applied to channels can improve performance. FractalNet [20] proposes to randomly drops individual paths during training, and Stochastic depth [15] randomly drops a subset of layers and forwards inputs with residual connection during training. These dropout variants apply dropout to the basic components of CNNs, e.g., channels and paths, which regularizes CNNs for improved training.

### 3 DROPOUT FOR DEEP CONVOLUTIONAL NEURAL NETWORKS

In this section, we first formulate the basic transformations of Convolutional Neural Networks from the viewpoint of split-transform-aggregate. We then introduce general training mechanisms with dropout operations at different structural levels for CNNs. We also examine various CNN architectures and propose convolutional building blocks with dropout training that are better in line with the dropout mechanisms for more efficient and effective regularization.

#### 3.1 The Basic Transformations of CNNs

Broadly speaking, the topology of neural networks, including multi-layer perceptron, recurrent neural networks [11] and convolutional neural networks [19], [7], [14], can be represented precisely by a set of neurons and their connections from the connectionist viewpoint, where the information flow from input neurons to output neurons is regulated by learnable weights of each connection. Succinctly, each neuron aggregates information from its input neurons by:

$$y_i = \sum_{j=1}^N w_{ij} x_j \quad (1)$$

where  $\mathbf{x} = [x_1, x_2, \dots, x_N]$  is a N-dimension input vector, and  $w_{ij}$  the weight of the connection from input neuron  $x_j$  to the output neuron  $y_i$ . We omit bias and output nonlinearity here for brevity. The neuron transformation follows the strategy of split-transform-aggregate, which can be interpreted as extracting features from all the input branches by first the dot product transformation of the input information with corresponding weights and then an aggregation over the input dimensions.

The transformation of convolutional neural networks can be formulated at a higher structural level with channels as the basic components instead of neurons. Specifically, the most fundamental operation in CNNs comes from the convolutional layer which can be constructed to represent any given transformation  $\mathcal{F}_{conv} : \mathbf{X} \rightarrow \mathbf{Y}$ , where  $\mathbf{X} \in \mathbb{R}^{C_{in} \times W_{in} \times H_{in}}$  is the input with  $C_{in}$  channels of size  $W_{in} \times H_{in}$ , and  $\mathbf{Y} \in \mathbb{R}^{C_{out} \times W_{out} \times H_{out}}$  is the output likewise.

Denoting  $\mathbf{X}, \mathbf{Y}$  as  $[\mathbf{x}_1, \mathbf{x}_2, \dots, \mathbf{x}_{C_{in}}], [\mathbf{y}_1, \mathbf{y}_2, \dots, \mathbf{y}_{C_{out}}]$  in vector of channels respectively, the parameter set associated with this convolutional layer comprises a series of filter kernels  $\mathbf{W} = [\mathbf{w}_1, \mathbf{w}_2, \dots, \mathbf{w}_{C_{out}}]$ . Then the convolutional transformation on  $\mathbf{X}$  can be succinctly represented as:

$$\mathbf{y}_i = \mathbf{w}_i * \mathbf{X} = \sum_{j=1}^{C_{in}} \mathbf{w}_i^j * \mathbf{x}_j \quad (2)$$

where  $*$  denotes convolution operation, and  $\mathbf{w}_i^j$  is a 2D spatial kernel associated with  $i_{th}$  output channel  $\mathbf{y}_i$  and convolves on  $j_{th}$  input channel  $\mathbf{x}_j$ . For a typical convolutional layer, each output channel  $\mathbf{y}_i$  is connected to all the input channels  $\mathbf{X}$  and is typically followed by some output nonlinearity, which is omitted here for succinctness.

We argue that the channel level representation more natural to the convolutional transformation of CNNs. Structurally, CNNs consist of a stack of convolutional layers and for each convolutional layer, the transformation convolves over channels as in Equation 2. Unlike dense layers such as fully connected layers where each connection between input and output neurons is coupled with one learnable weight, neurons within the same channel share the same filter kernel for each output channel in CNNs. Such a weight sharing strategy dramatically reduces the number of parameters of CNNs and suggests that CNNs extract features at the channel level. This is also supported by the visualization of convolutional kernels [19], [38], where filter kernels of the input-connected layer learn to identify orientations and colored blobs with increasing invariance, and class discrimination is observed ascending the layers.

#### 3.2 Dropout Operations for CNNs

In this subsection, we first outline mainstream convolutional transformations of representative CNN architectures. Next, different structural levels of dropout operations are introduced and examined to improve the training of CNNs. We then propose general convolutional building blocks integrated with built-in dropout operations and a more efficient and effective dropout variant drop-conv2d for CNNs.

##### 3.2.1 Convolution Transformation Blocks

We illustrate mainstream convolutional transformation in Figure 2. Conventional convolution transforms via the operation 2 and 4, namely an identity mapping of  $\mathbf{X}$  and then a convolutional transformation  $\mathcal{F}_{conv}$ , which follows the formulation in Equation 2. Other convolution transformations such as group convolution [19] and depth-wise convolution [12] can also be formulated accordingly with their respective constraints on channel connections.

Many convolutional transformations try to lengthen and/or widen the transformation. For instance, NIN [22]

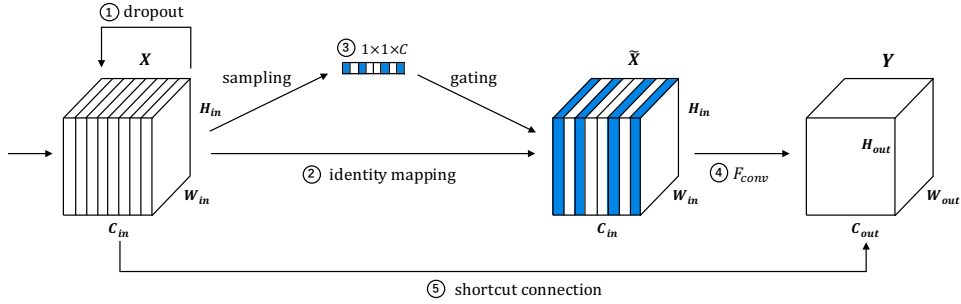


Fig. 2: Illustration of various convolutional transformations. Dropout, or drop-neuron, gates input neurons in operation 1; Drop-channel replaces identity mapping in operation 2 with operation 3, random sampling and gating on channels; Drop-path is introduced to  $\mathcal{F}_{conv}$  in operation 4 or to the shortcut connection in operation 5 (Drop-Layer).

lengthens  $\mathcal{F}_{conv}$  by following the filter kernel with two layers of multilayer perceptron transformation, which is structurally equivalent to two convolutional layers with  $1 \times 1$  filter. Inception series [29], [28] widen  $\mathcal{F}_{conv}$  with multiple heterogeneous transformation branches. ResNeXt [35] follows similar strategy by duplicating it  $P$  times  $\mathcal{F}_{conv}(\mathbf{X}) = \sum_{i=1}^P \mathcal{F}_{conv}_i(\mathbf{X})$ , where the transformations are heterogeneous. Other convolutional transformations encourage feature reuse by forwarding input channels  $\mathbf{X}$  directly to output channels  $\mathbf{Y}$ , as is indicated in operation 5. One commonly-adopted feature reuse is the shortcut of identity mapping proposed in ResNet [7], [8], i.e.  $\mathbf{Y} = \mathcal{F}_{conv}(\mathbf{X}) + \mathbf{X}$ . The shortcut structure facilitates gradient backpropagation and encourages residual learning. DenseNet [14] instead proposes direct feature reuse by forwarding and appending input channels  $\mathbf{X}$  directly to  $\mathbf{Y}$ , specifically  $\tilde{\mathbf{Y}} = [\mathbf{X}; \mathbf{Y}]$ .

### 3.2.2 Drop-neuron - The Neuron Level Dropout

Dropout [27], [10] is widely adopted in the training of deep neural networks as an effective regularization and implicit model ensemble method. The standard dropout is applied to each input neuron with a single parameter  $p$  during training, controlling the participation of each neuron  $x_j$  with a gating variable  $\alpha_j$  for each forward pass:

$$y_i = \frac{1}{p} \sum_{j=1}^N w_{ij} (\alpha_j \cdot x_j), \alpha_j \sim \text{Bernoulli}(p) \quad (3)$$

where  $\cdot$  denotes scalar multiplication and  $\alpha_j$  is an *independent* Bernoulli random variable which takes the value 1 with probability  $p$  (the retain ratio) and the value 0 with probability  $q = 1 - p$  (the drop ratio). The scaling factor  $\frac{1}{p}$  scales the output activation to keep the expected value of the output during training. Then during inference, the transformation is simply the same as Equation 1. We name the neuron level dropout drop-neuron to distinguish it from other higher structural levels of dropout variants. Drop-Neuron introduces randomness to the training process, which forces each neuron to learn more robust representations that are effective with varying input neuron set, and thus improves generalization. Therefore, the resultant network for inference can be regarded as an exponentially-sized ensemble of all possible subnets.

As illustrated in the operation 1 of Figure 2, drop-neuron empirically proves to be effective for deep neural networks, especially for dense layers such as fully-connected layers and recurrent layers. However, recent CNN architectures [7], [14], [13] find that dropout is ineffective for convolutional layers. We note that this can be attributed to the fact that in convolutional layers, neurons within the same input channel are highly spatial correlated, and features are extracted channel-wise. Therefore, dropping neurons independently can hardly regularize the training of deep CNNs, whose effectiveness is further reduced when CNNs train with extensive data augmentation.

### 3.2.3 Drop-Channel- The Channel Level Dropout

The channel level dropout, i.e., drop-channel, is inspired by the observation that there exists a close structural correspondence between channels in the convolutional layer and neurons in canonical neural networks, which is formulated formally in Equation 1 and Equation 2. Therefore, dropping channels should be structurally more effective in regularization. Following a similar methodology, drop-channel can be formulated as:

$$\mathbf{y}_i = \mathbf{w}_i * \tilde{\mathbf{X}} = \frac{1}{p} \sum_{j=1}^{C_{in}} \mathbf{w}_i^j * (\alpha_j \cdot \mathbf{x}_j) \quad (4)$$

where  $\alpha_j$  is again an *independent* Bernoulli random variable with probability  $1 - p$  of being 1 and is applied to the entire channel  $\mathbf{x}_j$ . Particularly,  $\alpha_j$  controls the presence of the input channel  $x_j$  during training. The drop-channel training is illustrated in Figure 2, where the identity mapping of operation 2 is replaced by operation 3, a random sampling of  $\alpha_j$  followed by the corresponding gating on input channels. The scaling factor  $\frac{1}{p}$  here again compensates for the scale loss from the deactivation of input channels and keeps the expected value of the output during training. The resultant network after training can then be directly used for inference with Equation 2.

The idea of channel level dropout is first introduced in SpatialDropout [30]. However, [30] only shows that SpatialDropout improves CNN models over an object localization dataset, and the effectiveness of SpatialDropout in interaction with other training techniques, e.g., data augmentation and batch normalization [16], are not investigated. To

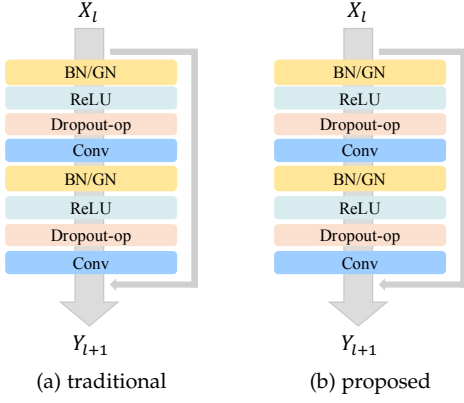


Fig. 3: The convolutional building blocks with drop-operations, for both drop-neuron and drop-channel, demonstrated with the pre-activation residual convolution block.

better harness the regularization and ensemble effects, we examine the complex interaction between drop-channel and these techniques extensively used in state-of-the-art CNNs theoretically and empirically.

$$\hat{\mathbf{x}}_j = \frac{\mathbf{x}_j - \mu_j}{\sqrt{\sigma_j^2 + \epsilon}}; \mathbf{x}'_j = \gamma_j \hat{\mathbf{x}}_j + \beta_j \quad (5)$$

Each convolutional layer of deep CNNs is typically followed with a batch normalization layer (BN) [16] to normalize inputs batch-wise, which stabilizes the mean and variance of the input channels  $\mathbf{X}$  received by each output channel  $\mathbf{y}_i$ . Take the pre-activation convolutional layers [8], [14], [13] for example, the convolutional transformation follows the *BN-ReLU-Conv* transformation pipeline, as illustrated in Figure 3a. We note that the dropout operation, including drop-neuron and drop-channel, is not integrated into the convolutional blocks properly, which is either totally discarded in recent CNNs or used in an erroneous way. As shown in Equation 5, the BN layer normalizes each input channel  $\mathbf{x}_j$  with the batch channel mean  $\mu_j$  and variance  $\sigma_j$ , and keeps running estimates of them, which will be directly used for the normalization of the  $j_{th}$  input channel after training.  $\gamma_j$  and  $\beta_j$  are learnable affine transformation parameters associated with channel  $\mathbf{x}_j$ , and  $\epsilon$  is for computation stability.

However, the two dropout operations are traditionally introduced right between the convolutional layer and the BN layer, which leads to violent fluctuation of the mean and variance of inputs received by the BN layer, for both drop-neuron and drop-channel. We attribute the failure of the traditional drop-neuron and drop-channel to the incorrect placement of the dropout operations and propose general convolutional building blocks with the dropout operations placed right before each convolutional layer in Figure 3b. Integrating drop-operations before the convolutional operation, as is also analyzed in the local reparameterization of the variational dropout [17], leads to lower gradient variance and thus faster convergence. In Section 4, we will also validate empirically the effectiveness of the proposed

convolutional blocks on various state-of-the-art CNNs with extensive experiments.

The disharmony between drop-neuron and the BN layer has also been analyzed in [21], which shows that there exists inconsistency of the variance estimation of BN from training to inference when the BN layer coupled with the neuron level dropout. The variance shift leads to unstable predictions and thus probably worse inference performance. A simple way to reduce this issue is to update the variance estimation [9] of BN layers after training without dropout. In this paper, we further formally examine drop-channel and show that for CNNs, variance shift can be largely reduced with dropout operations placing right before the convolutional layer. In CNNs, inputs are normalized channel-wise, and different channels transform with different filters. Particularly, each channel  $\mathbf{x}_j$  of the input  $\mathbf{X}$  is obtained by convolution over inputs of its preceding layer with an independent filter, whose mean and variance are then subsequently normalized with BN independently of other channels. Therefore, we can denote that the  $j_{th}$  input channel  $\mathbf{x}_j$  shares the same mean  $\beta_j$  and variance  $\gamma_j^2$  (i.e.  $E(x_{j,\cdot}) = \beta_j$  and  $\text{Var}(x_{j,\cdot}) = \gamma_j^2$ ), and assume uncorrelatedness between different channels (i.e.  $\text{Cov}(x_{i,\cdot}, x_{j,\cdot}) = 0, i \neq j$ )<sup>2</sup>. Then for drop-channel in the traditional block, dropout operates on  $\mathbf{y}_i$  as in Equation 2 (the input  $\mathbf{x}_i$  of the next layer), and outputs  $y'_{i,k} = \frac{1}{p} \alpha_i y_{i,k}$  during training. Denoting  $E(\mathbf{y}_{i,\cdot}) = \beta_i$  and  $\text{Var}(\mathbf{y}_{i,\cdot}) = \gamma_i^2$ , and omitting subscript  $i, k$ , we have:

$$\begin{aligned} \text{Var}^{Train}(y') &= \frac{1}{p^2} E(\alpha^2) E(y^2) - \frac{1}{p^2} (E(\alpha) E(y))^2 \\ &= \frac{1}{p} \gamma^2 + \frac{1-p}{p} \beta^2 \end{aligned} \quad (6)$$

Conventionally, the BN layer following  $\mathbf{y}_i$  keeps a record of the variance  $\text{Var}^{Train}(y'_i)$  and uses the running estimate of it during inference. This variance estimation deviates from the actual variance  $\text{Var}^{Test}(y') = \gamma^2$ , and the shift ratio is:

$$\Delta(p)' = \frac{\text{Var}^{Train}(y')}{\text{Var}^{Test}(y')} = \frac{1}{p} + \frac{1-p}{p} \frac{\beta^2}{\gamma^2} \quad (7)$$

Therefore, there exists a variance shift of ratio  $\Delta(p) \geq 1$ , and  $\Delta(p) = 1$  only when the channel retain ratio  $p$  is 1, i.e., the absence of dropout operation. In the proposed convolutional building block, dropout instead operates on  $\mathbf{x}_i$  as in Equation 4 right after the convolution operation. We first vectorize the filter for each input channel  $\mathbf{x}_i$ ; then for each output  $y_{i,k}$  of  $\mathbf{y}_i$ , we have  $y_{i,k} = \frac{1}{p} \sum_{j=1}^{C_{in}} \sum_{d=1}^D w_{i,d}^j \cdot (\alpha_j \cdot x_{j,k*d})$ , where  $x_{j,k*d}$  denotes the vectorized receptive field of  $y_{i,k}$ . Omitting the subscript  $i, k$  and with uncorrelatedness we have:

$$\begin{aligned} \text{Var}^{Train}(y) &= \frac{1}{p^2} \sum_{j=1}^{C_{in}} \text{Var}[\alpha_j \sum_{d=1}^D (w_d^j x_{j,d})] \\ &= \frac{1}{p} \text{Var}^{Test}(y) + \frac{1-p}{p} \sum_{j=1}^{C_{in}} \beta_j^2 \left( \sum_{d=1}^D w_d^j \right)^2 \end{aligned} \quad (8)$$

2. In practice, obtaining fully uncorrelatedness requires expensive input whitening on the input  $\mathbf{X}$ .

where the inference variance is:

$$\begin{aligned} \text{Var}^{Test}(y) &= \sum_{j=1}^{C_{in}} \text{Var}\left(\sum_{d=1}^D (w_d^j x_{j,d})\right) \\ &= \sum_{j=1}^{C_{in}} \gamma_j^2 \sum_{m=1}^D \sum_{n=1}^D w_m^j w_n^j \rho_{m,n}^j \end{aligned} \quad (9)$$

where  $\rho_{m,n}^j = \frac{\text{Cov}(x_{j,m}, x_{j,n})}{\sqrt{\text{Var}(x_{j,m})}\sqrt{\text{Var}(x_{j,n})}} \in [-1, 1]$  measures the linear correlation between  $x_{j,m}$  and  $x_{j,n}$ . Therefore, the shift ratio of the proposed drop-channel block is:

$$\begin{aligned} \Delta(p) &= \frac{\text{Var}^{Train}(y)}{\text{Var}^{Test}(y)} \\ &= \frac{1}{p} + \frac{1-p}{p} \frac{\sum_{j=1}^{C_{in}} \beta_j^2 \sum_{m=1}^D \sum_{n=1}^D w_m^j w_n^j}{\sum_{j=1}^{C_{in}} \gamma_j^2 \sum_{m=1}^D \sum_{n=1}^D w_m^j w_n^j \rho_{m,n}^j} \end{aligned} \quad (10)$$

We note that although  $\Delta(p) \geq 1$ , the variance shift of drop-channel after the convolution is smaller and more stable than  $\Delta(p)'$ . For  $\Delta(p)'$ , the  $\beta_j$  and  $\gamma_j^2$  are the mean and variance of the channel activations after the convolution, which keeps evolving during the training process and could be unbounded. In contrast, for  $\Delta(p)$ ,  $\beta_j$  and  $\gamma_j^2$  are typically the mean and variance of the channel activations normalized by its preceding BN layer and is thus stable; and the kernel weight  $w_{i,d}^j$  and the correlation between input  $x_{j,m}$  and  $x_{j,n}$  in the same channel  $\mathbf{x}_j$  are also relatively stable as the training progresses.

Empirically, we observe less variance shift with drop-channel placed right before the convolutional layer and with a relatively large channel retain ratio (e.g., 0.9), whose shift ratio is rather close to BN training without dropout. We note that the variance shift of drop-channel can be greatly reduced by updating BN running estimates after training, and alternatively, the regularization and implicit model ensemble benefits from drop-channel can be fully harnessed by replacing BN with Group Normalization [34] (GN). GN normalizes channels within the same channel group of each layer instead of batch-wise as in BN, and requires no running estimates of the channel mean and variance and thus leads to no variance shift. Compared with drop-neuron, CNNs trained with our proposed drop-channel generally improve training considerably.

### 3.2.4 Higher Level Dropouts: Drop-paths

The path level dropout drop-path are introduced in FractalNet [20]. Notably, ResNet with Stochastic Depth [15] proposes to randomly drop the residual path and forward the input  $\mathbf{X}$  during training with the shortcut connection of operation 5, which is denoted as drop-layer and can be regarded as a drop-path that randomly drops the transformation path. Formally, drop-path can be formulated as:

$$\mathbf{Y} = \mathcal{F}_{conv}(\mathbf{X}) = \frac{1}{p} \sum_{i=1}^P \alpha_i \cdot \mathcal{F}_{conv\_i}(\mathbf{X}) \quad (11)$$

where  $P$  is the number of paths (branches) of the convolutional layer, and  $\alpha_i$  is a Bernoulli gating variable that controls the participation of  $i_{th}$  path in the transformation with

the retain ratio  $p$ . Although drop-path and drop-layer are effective in regularizing CNNs, they are highly dependent on CNN architectures. Specifically, drop-path requires CNN to contain multiple paths, either homogeneous or heterogeneous, of  $\mathcal{F}_{conv}$  in operation 4; and particularly, drop-layer demands shortcut connection of operation 5 illustrated in Figure 2. In FractalNet, drop-path is applied to the fractal architecture, whose paths are heterogeneous.

We note that drop-path can be integrated as a general building block with the bottleneck structure [7] and group convolution [19]. Specifically, the building block is based on the bottleneck structure of one  $3 \times 3$  convolution surrounded by dimensionality reducing and expanding with a  $1 \times 1$  convolution, i.e.,  $conv1 \times 1 - conv3 \times 3 - conv1 \times 1$ . To support drop-path, group convolution is introduced to the inner  $3 \times 3$  convolutional layer with  $P$  groups as proposed by ResNeXt [35]. Then structurally, the bottleneck building block contains  $P$  independent paths of homogeneous transformations, each of which first collapses  $C$  input channels into  $d$  channels by a  $1 \times 1$  convolution, and then transforms by an inner  $3 \times 3$  convolution within each path and finally expands back to  $C$  channels by a  $1 \times 1$  convolution. In this implementation, such a building block is equivalent to the bottleneck with the inner  $3 \times 3$  convolution of  $P$  groups. We further propose to choose  $P$  to be a power of 2 empirically, e.g., 16, 32, 64 and fix  $P$  for the whole network, and  $d = \frac{C}{2^P}$ . Further, we find that drop-layer is better in line with the shortcut connection of identity mapping [8], [37], i.e.,  $\mathbf{Y} = \mathcal{F}_{conv}(\mathbf{X}) + \mathbf{X}$ , where output scaling is not needed since the residual path  $\mathcal{F}_{conv}(\mathbf{X})$  for random dropping is pushed towards zero [7].

### 3.2.5 Dropout as General Training Regularization for CNNs

Thus far, we have formulated and examined three different structural levels of dropout, i.e., drop-neuron, drop-channel and drop-path. The effectiveness of different dropout variants can be mainly attributed to the regularization and ensemble effect [10], [32], [27]. We note that drop-neuron and drop-channel are readily applicable to existing CNNs with the adjustment of placing the dropout operation right before each convolutional transformation; we have also proposed corresponding building blocks with drop-neuron/drop-channel in Section 3.2.3 and drop-path in Section 3.2.4.

Inspired by drop-channel (Equation 4) and drop-path (Equation 11), we further propose Drop-Conv2d for CNNs as a general regularization technique, which treats each channel connection between input and output channels as a channel path and then replicates each path  $P$  times:

$$\begin{aligned} \mathbf{y}_i &= \tilde{\mathbf{w}}_i * \mathbf{X} = \sum_{j=1}^{C_{in}} \left(\frac{1}{p} \alpha_j \cdot \mathbf{w}_i^j\right) * \mathbf{x}_j \\ &= \sum_{j=1}^{C_{in}} \left(\sum_{k=1}^P \frac{1}{p} \alpha_{j,k} \cdot \mathbf{w}_i^{j,k}\right) * \mathbf{x}_j \end{aligned} \quad (12)$$

where  $P$  is the number of path replicates for each channel connection, and  $\alpha_{j,k}$  is again an independently sampled Bernoulli gating variable. In implementation, Equation 4 of drop-channel can be equivalently regarded as convolution over each input channel  $\mathbf{x}_j$  with dropout weight  $\tilde{\mathbf{w}}_i^j = \frac{1}{p} \alpha_j \cdot \mathbf{w}_i^j$ , where the coefficient  $\frac{1}{p} \alpha_j$  is the scaling factor

during training. For drop-conv2d, we enhance each channel path with an ensemble of  $P$  paths of different weights during training, i.e.  $\mathbf{w}_i^j = \sum_{k=1}^P \mathbf{w}_i^{j,k}$ , and scale each weight  $\mathbf{w}_i^{j,k}$  with dropout scaling factor  $\frac{1}{P} \alpha_{j,k}$  accordingly.

We note that the drop-conv2d enhancement leads to both larger model capacity and better dropout training, harnessing regularization and model ensemble benefits for improved training. More importantly, such enhancement incurs negligible costs. Specifically, during training, we only need to replicate the weights  $P$  times, and the convolution of inputs with these weights can be equivalently implemented by first a weighted average of these weights and then the computational heavy convolution. Then during inference, the  $P$  channel weights can be aggregated back into one, and the convolution with drop-conv2d is therefore the same as the one trained without drop-conv2d. We further note that these dropout variants (particularly drop-conv2d) can be readily integrated into deep CNNs by simply replacing the convolutional blocks with our proposed ones and then configuring the dropout rate for the required regularization strength, which generally takes no additional model parameter and incurs negligible computational cost while effectively improve the training of CNNs. Further, these dropout variants can be jointly adopted in CNNs whenever possible, e.g., drop-channel, drop-path can be adopted in ResNeXt [35] concurrently.

## 4 EXPERIMENTS

The four structural levels of dropouts are evaluated on representative CNNs on widely benchmarked datasets, including CIFAR, SVHN and ImageNet. We first introduce the dataset and training details and CNN architectures. We then evaluate the effectiveness of our building blocks with the proposed dropout operations. We compare drop-neuron, drop-channel, drop-path (also drop-layer), drop-conv2d and their combinations, with which we improve over state-of-the-art CNNs on CIFAR and SVHN datasets and achieve consistently better results.

### 4.1 Dataset Details

#### 4.1.1 CIFAR

The two CIFAR [18] datasets consist of  $32 \times 32$  colored scenery images. CIFAR-10 (C10) consists of images drawn from 10 classes, and CIFAR-100 (C100) from 100 classes. The training and testing set for both datasets contain 50,000 and 10,000 images respectively. Following the standard data augmentation scheme [7], [15], [14], each image is first zero-padded with 4 pixels on each side, then randomly cropped to produce  $32 \times 32$  images again, followed by a random horizontal flip. We denote the datasets with data augmentation with "+" behind the dataset names (e.g., C10+). We normalize the data using the channel means and standard deviations for data preprocessing.

#### 4.1.2 SVHN

The Street View House Numbers dataset [24] contains  $32 \times 32$  colors digit images from Google Street View. The task is to correctly classify the central digit into one of the 10

digit classes. The training and testing sets respectively contain 73,257 and 26,032 images, and an additional training dataset contains 531,131 images that are relatively easier to classify. We adopt a common practice [15], [37], [14] by using all the training data without any data augmentation. Following [37], [14], we divide each pixel value by 255, scaling the input to range [0, 1].

#### 4.1.3 ImageNet

The ILSVRC 2012 image classification dataset contains 1.2 million images for training and 50,000 for validation from 1000 classes. We adopt the same data augmentation scheme for training images following the convention [7], [37], [14], and apply a  $224 \times 224$  center crop to images at test time. The results are reported on the validation set.

## 4.2 CNN Architecture Details

As discussed in Section 3.2.5, drop-neuron and drop-channel are generally applicable to CNNs, while the applicability of drop-path and drop-layer are dependent on CNN architectures. To evaluate the effectiveness of these dropout variants, we adopt CNN architectures with representative convolutional transformation.

Specifically, we first evaluate and compare drop-neuron and drop-channel with our proposed building blocks illustrated in Figure 3b on VGG [26], whose convolutional layer is a plain  $3 \times 3$  conv following operation 2 and 4 of Figure 2. For drop-path of the new building block proposed in Section 3.2.4 and drop-layer, we validate their effectiveness in comparison with drop-channel and drop-neuron on ResNeXt [35] with (1) multiple paths and residual connection, (2) Wide Residual Networks [37] (WRN) with wider convolutional layer and residual connection and (3) DenseNet [14] with shortcut connection.

We denote these models with WRN-depth-k, ResNeXt-depth-P-d and DenseNet-L-K, with k, P, d, L, K as the widening factor [37], the number of paths, the channel width of each path [35], the number of layers (depth) and K the growth rate [14], respectively. The building blocks of WRN, ResNeXt and DenseNet are basic block (Block) with two consecutive  $3 \times 3$  conv, the bottleneck block (B-Block) proposed in Section 3.2.4 and the DenseNet bottleneck block (D-Block) [14] with dimensionality reduction of  $1 \times 1$  conv and the following transformation of  $3 \times 3$  conv. The detailed model configurations for CIFAR-10/100, SVHN and ImageNet datasets are introduced in Table 1 and Table 2.

For CNNs trained with drop-neuron and drop-channel, each convolutional layer is replaced with the proposed building block in Section 3.2, where the dropout operations are integrated into the transformation right before the convolution. While for drop-path, each convolutional layer is replaced with the proposed general drop-path building block in Section 3.2.4.

### 4.3 Training Details

For all the experiments, we train the CNNs with SGD and Nesterov momentum. For CIFAR datasets, we train 300 epochs for VGG-11, ResNeXt-29-P64-d4 and DenseNet-L190-K40, and 200 epochs for WRN-40-4. For SVHN, we train 160 epochs for WRN-16-8. The initial learning rate is

Group	Output Size	VGG-11	WRN-16-8	ResNeXt-29-P64-d4	DenseNet-L190-K40	WRN-40-4
conv1	32×32	[conv3×3, 64]×2	[conv3×3, 16]×1	[conv3×3, 64]×1	[conv3×3, 80]×1	[conv3×3, 16]×1
conv2	32×32	-	[Block, 16×4]×6	[B-Block, 256]×4	[D-Block, 80-1320]×31	[Block, 16×8]×2
conv3	16×16	[conv3×3, 256]×2	[Block, 32×4]×6	[B-Block, 512]×4	[D-Block, 660-1900]×31	[Block, 32×8]×2
conv4	8×8	[conv3×3, 256]×2	[Block, 64×4]×6	[B-Block, 1024]×4	[D-Block, 950-2190]×31	[Block, 64×8]×2
conv5	8×8	[conv3×3, 512]×4	-	-	-	-
avgPool	1×1	[avg8×8, 512]	[avg8×8, 256]	[avg8×8, 1024]	[avg8×8, 2190]	[avg8×8, 512]
Dataset	-	CIFAR	CIFAR	CIFAR	CIFAR	SVHN
Params	-	9.89M	8.95M	8.85M	25.62M	10.96M

TABLE 1: Detailed architectures and configurations of representative convolutional neural networks for CIFAR and SVHN datasets. Building blocks are denoted as “[block, number of channels] × number of blocks”.

Group	Output Size	VGG-16	Output Size	WRN-50-2	DenseNet-L169-K32
conv1	224×224	[conv3×3, 64]×2	112×112	conv7×7, stride 2	conv7×7, stride 2
pooling	112×112	2×2 max pool, stride 2	56×56	3×3 max pool, stride 2	3×3 max pool, stride 2
conv2	112×112	[conv3×3, 128]×2	56×56	[B-Block, 64×2]×6	[D-Block, 64-256]×6
pooling	56×56	2×2 max pool, stride 2	28×28	conv3×3, stride 2	Transition Layer
conv3	56×56	[conv3×3, 256]×2	28×28	[B-Block, 128×2]×3	[D-Block, 128-512]×12
pooling	28×28	2×2 max pool, stride 2	14×14	conv3×3, stride 2	Transition Layer
conv4	28×28	[conv3×3, 512]×2	14×14	[B-Block, 256×2]×3	[D-Block, 256-1792]×32
pooling	14×14	2×2 max pool, stride 2	7×7	conv3×3, stride 2	Transition Layer
conv5	14×14	[conv3×3, 512]×2	7×7	[B-Block, 512×2]×3	[D-Block, 896-1920]×32
pooling	7×7	2×2 max pool, stride 2	1×1	7×7, global avg-pool	7×7, global avg-pool
FC	1000	[512×7×7, 4096, 4096, 1000]	1000	[1024, 1000]	[1920, 1000]
Params	-	138.4M	-	68.9M	14.1M

TABLE 2: Detailed configurations of representative CNNs for the ImageNet dataset.

set to 0.1, weight decay 0.0001, dampening 0, momentum 0.9 and mini-batch size 128 for CIFAR and SVHN datasets. The learning rate is divided by 10 at 50% and 75% of the total number of training epochs. For ImageNet, we train 100 epochs for VGG-16, WRN-50-2 and DenseNet-L169-K32 with a mini-batch size of 128. The initial learning rate is set to 0.05, and is lowered by a factor of 10 after epoch 30, 60 and 90. We use a weight decay of 0.0001 and momentum 0.9 without dampening.

## 4.4 Experimental Results

### 4.4.1 Building Blocks of Drop-Neuron and Drop-Channel

Network	original	DN	DN+	DC	DC+
VGG	5.09	5.18	4.98 (+0.20)	4.78	<b>4.67 (+0.11)</b>
WRN	4.97	4.89	4.63 (+0.26)	4.60	<b>4.31 (+0.29)</b>
DenseNet	4.57	4.70	4.52 (+0.18)	4.56	<b>4.32 (+0.24)</b>

TABLE 3: Error rates (%) of CNNs trained with dropout operations w/ and w/o the proposed blocks on CIFAR-10.

We validate the effectiveness of the proposed building blocks supporting drop-neuron and drop-channel on VGG-11, WRN-40-4 and DenseNet-L100-K12, as introduced in Section 4.2 and Table 1. The results are summarized in Table 3, where we report the results of networks trained without dropout (original), with traditional drop-neuron and drop-channel (DN and DC), and with the proposed drop-neuron and drop-channel (DN+ and DC+) respectively.

We can notice that the proposed building blocks consistently improve over the original blocks by a significant margin. Comparing to the original results, networks trained with drop-neuron and drop-channel achieve significantly better performance, which demonstrates that the dropout technique is effective in regularizing CNNs if applied properly. For instance, the introduction of drop-channel alone achieves a reduction of the error rate by 0.42%, 0.66% and 0.25% on VGG-11, WRN-40-4 and DenseNet-L100-K12 respectively.

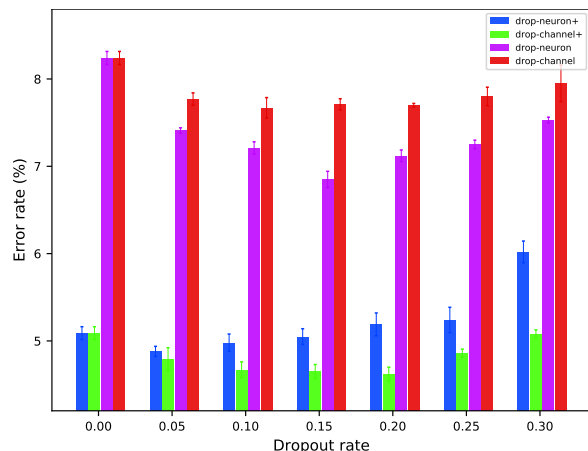


Fig. 4: Error rate (%) of VGG-11 trained with drop-neuron and drop-channel w/ and w/o data augmentation.

### 4.4.2 Dropout operations and Data Augmentation

We evaluate the relationship between data augmentation and dropout operations of drop-neuron and drop-channel for CNNs. The results are reported on VGG-11, whose error rates and learning curves are illustrated in Figure 4 and Figure 5. We denote VGG networks trained without dropout, with drop-neuron and drop-channel as VGG-11, drop-neuron and drop-channel respectively, and the network trained with standard data augmentation is marked with a suffix +.

We summarize the main results in Figure 4, where error rates and standard deviations are reported with the dropout rate in every 0.05. The results show that data augmentation is essential for CNNs; without data augmentation, the performance decreases by around 3%. Further, drop-neuron and drop-channel improve the performance noticeably both with and without data augmentation. With data augmentation and drop-channel, the model achieves the best result of 4.62% from 8.24%, i.e., a 3.62% error rate reduction; mean-

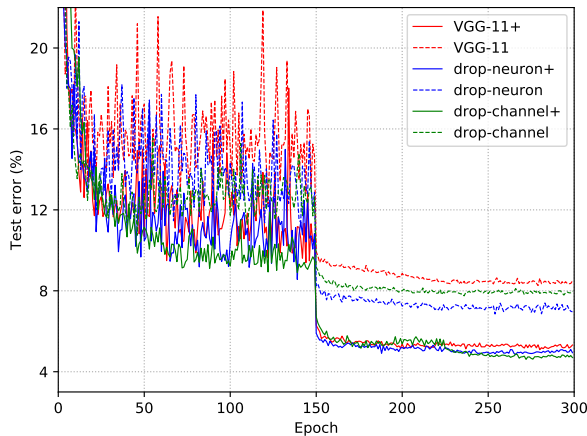


Fig. 5: Learning curves of VGG-11 trained w/ and w/o drop-neuron, drop-channel and data augmentation.

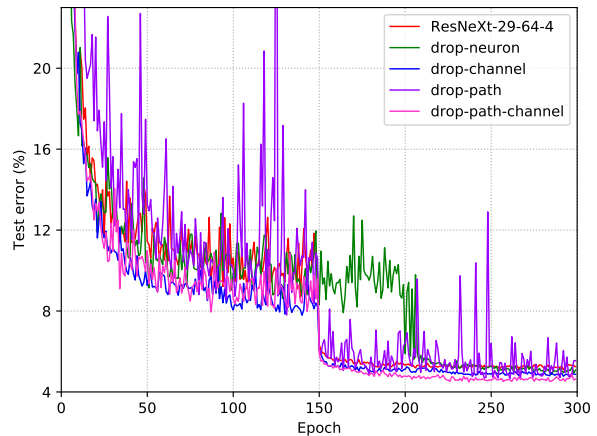


Fig. 7: Learning curves of ResNeXt-29-64-4 trained with drop-neuron, drop-channel and drop-path.

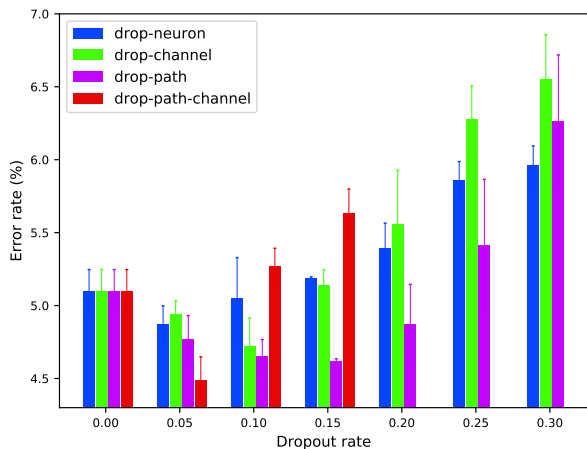


Fig. 6: Error rate (%) of ResNeXt-29-64-4 trained with drop-neuron, drop-channel and drop-path.

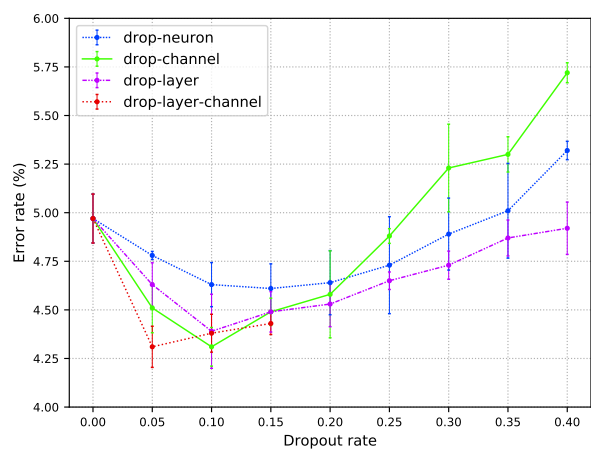


Fig. 8: Error rate (%) of WRN-40-4 trained with drop-neuron, drop-channel and drop-layer.

while without data augmentation, drop-neuron achieves a better result of 6.85% than drop-channel. These results show that the regularization effect of drop-neuron overlaps with data augmentation to some extent.

We further plot learning curves of CNNs trained with the best dropout rates in Figure 5. The learning curves confirm these findings and demonstrate that drop-neuron and drop-channel are indeed effective in regularizing CNNs. For state-of-the-art CNNs trained with extensive data augmentation, drop-channel is more effective in regularization, which improves the performance by a noticeable margin.

#### 4.4.3 The effectiveness of Drop-Path and Drop-Layer

We evaluate drop-path on ResNeXt-29-64-4 (see Table 1), specifically the effect of drop-path alone and with other dropout operations. We adopt building blocks supporting drop-path as proposed in Section 3.2.4.

The results of ResNeXt trained with drop-neuron, drop-channel, drop-path and dropout with both drop-path and drop-channel (drop-path-channel, with the same dropout rate from 0.05 to 0.15) are summarized in Figure 6. Results show that drop-neuron reduces the error rate modestly from 5.10% to 4.87%, and drop-channel outperforms drop-neuron with a lower error rate of 4.72%. With the proposed

drop-path building block, ResNeXt achieves a better result of 4.62%, i.e., a 0.48% relative reduction over the network without dropout.

As discussed in Section 3.2.5, the path level dropout can be adopted with finer-grained dropout operations, i.e., drop-neuron and drop-channel. With both drop-path and drop-channel, ResNeXt achieves the lowest error rate of 4.49% with a dropout rate of 0.05. This result confirms that different structural levels of dropouts can further improve the training of CNNs.

To understand the impact of dropouts on the training process, we plot the learning curves trained with different dropout variants in Figure 7. We can notice that firstly, CNNs trained with different dropout operations achieves noticeably better results than the network without dropout. Interestingly, the learning curve of networks with drop-path fluctuates drastically, though it achieves a lower error rate than other dropout variants. However, when trained with drop-channel, the training is more stable, and such integration yields the overall best result of a 4.49% test error rate. We conjecture that this is mainly because drop-path is a more radical regularization method, where each entire path is randomly dropped, and thus has higher variance. Therefore, drop-path may need a lower dropout rate.

Model	Depth	Params	C10	C10+	C100	C100+	SVHN
VGG [26]	11	9.89M	8.24	5.09	23.58	32.08	-
↳with drop-neuron	11	9.89M	4.88	6.85	23.15	27.71	-
↳with drop-channel	11	9.89M	4.62	7.76	21.89	29.51	-
Wide ResNet [37]	40	8.95M	-	4.97	-	-	-
↳with drop-neuron	40	8.95M	-	4.61	-	-	-
↳with drop-channel	40	8.95M	-	4.31	-	-	-
↳with drop-layer	40	8.95M	-	4.39	-	-	-
Wide ResNet [37]	16	10.96M	-	-	-	-	1.54
↳with drop-neuron	16	10.96M	-	-	-	-	<b>1.44</b>
ResNeXt [35]	29	8.85M	-	5.10	-	-	-
↳with drop-neuron	29	8.85M	-	4.87	-	-	-
↳with drop-channel	29	8.85M	-	4.72	-	-	-
↳with drop-path	29	8.85M	-	4.62	-	-	-
DenseNet-BC (k=12) [14]	100	0.8M	5.92	4.51	24.15	22.27	1.76
↳with drop-channel	100	0.8M	5.59	4.24	23.73	20.75	1.65
DenseNet-BC (k=40) [14]	190	25.6M	-	3.46	-	17.18	-
↳with drop-neuron	190	25.6M	-	3.42	-	16.69	-
↳with drop-channel	190	25.6M	-	<b>3.17</b>	-	<b>16.15</b>	-

TABLE 4: Overall results reported in error rate (%) on CIFAR and SVHN datasets. A suffix + indicates standard data augmentation. Only results in Section 4 are provided for comparison. The overall best results are highlighted in **blue**.

Model	Depth	Params	ImageNet
VGG-16 [26]	16	138.4M	27.63
↳+drop-channel	16	138.4M	27.49
WRN-50-2 [37]	50	68.9M	21.91
↳+drop-layer+channel	50	68.9M	21.68
DenseNet-L169-K32 [14]	169	14.1M	23.62
↳+drop-path+channel	169	14.1M	23.47

TABLE 5: Comparison of Top-1 (single model and single crop) error rates on ImageNet classification dataset.

In particular, we further evaluate the effect of drop-layer with ResNet with Stochastic Depth [15], which is discussed in Section 3.2.4 and Section 3.2.5. We focus on comparing drop-layer with other dropout variants, namely drop-neuron and drop-channel. We adopt WRN-40-4 (see Table 1) with dropout rate from 0.0 to 0.40 in every 0.05. The main results are summarized in Figure 8. We find that dropout operations help obtain noticeably better results. Specifically, drop-channel achieves the best result of a 0.66% reduction of test error rate from 4.97% to 4.31%. When trained with drop-channel, drop-layer improves performance considerably, which is comparable to drop-channel alone. We therefore conjecture that drop-channel is a better dropout training choice, which achieves generally better results with more stable training.

#### 4.4.4 Dropout: Improvement over State-of-the-art CNNs

Thus far, we have examined the building blocks of different structural levels of dropout for regularizing the training of deep CNNs, and meanwhile evaluate the effectiveness of different dropout operations, i.e., drop-neuron, drop-channel, drop-path (and drop-layer) with extensive experiments. With these general and effective dropout training mechanisms, we can further improve the training of best-performing CNNs on benchmark datasets. The overall results on CIFARs and SVHN are summarized in Table 4.

For SVHN, WRN-16-8 (Table 1) originally achieves 1.54% error rate without data augmentation. We then introduce our proposed drop-neuron and drop-channel building blocks to WRN, and the results are summarized in Figure 9. The results confirm that drop-neuron is more effective in

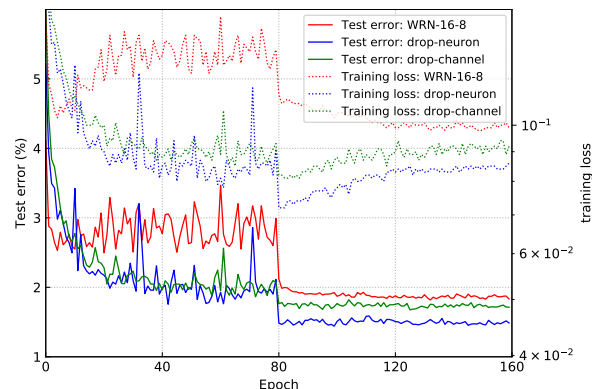


Fig. 9: Learning curves and losses of WRN-16-8 trained with drop-neuron, drop-channel on SVHN.

regularizing networks trained without data augmentation. Replacing conventional convolutional layers with the drop-neuron convolutional building blocks in WRN-16-8, we achieve a noticeably lower error rate of 1.44% on SVHN over the original state-of-the-art model. Figure 9 further shows that the proposed drop-neuron can effectively regularize the training process with a significantly lower training loss and meanwhile a lower error rate. Without dropout regularization, the training stagnates quickly, and the test error rate even increases and fluctuates dramatically before the first drop of the learning rate. While with dropouts, the training is more stable and the network continues to improve for lower errors.

For CIFAR datasets, the state-of-the-art model DenseNet-L190-K40 (see Table 1) achieves 4.36% and 17.18% error rate on CIFAR-10 and CIFAR-100 respectively. We then apply drop-neuron and drop-channel building blocks in replacement of convolutional layers in the network, and with a dropout rate 0.1, DenseNet-L190-K40 achieves significantly better results of 3.17% and 16.15% error rate, i.e., a 0.29% and 1.03% relative error rate reduction respectively.

The overall experimental results on ImageNet dataset are summarized in Table 5. Three representative CNN architectures are adopted for the large dataset, specifically VGG-

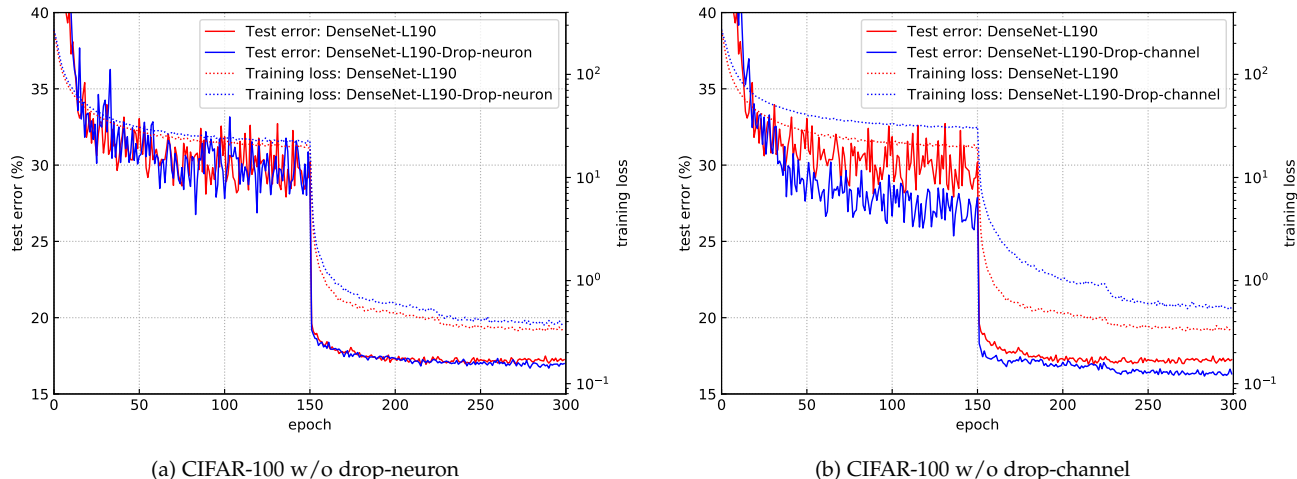


Fig. 10: Test error and training loss curves for DenseNet-L190-K40 with and without drop-neuron and drop-channel. The two corresponding dropout rates are both set to 0.1, leading to 16.76% and 16.15% test error rate respectively on CIFAR-100+. The test error is 17.18% for the network trained without any dropout.

16 [26] with the plain convolutional operation, WRN-50-2 [37] with residual connection and DenseNet-L169-K32 [14] with a dense connection between layers. We evaluate WRN-50-2 with both drop-layer and drop-channel, and meanwhile DenseNet-L169-K32 with both drop-path and drop-channel. For VGG-16, we improve accuracy by 0.14% with drop-channel. For WRN-50-2, we observe a more significant error rate reduction of 0.23% with the adoption of both drop-channel and drop-layer. With both drop-channel and drop-path training, DenseNet-L169-K32 obtains a 0.15% test error rate reduction. The results of the three architectures on ImageNet further confirm that the dropout training mechanisms can significantly improve the training of deep CNNs if adopted properly.

Finally, to illustrate the difference between the regularization effect of drop-neuron and drop-channel, we further plot training curves of the 190 layer DenseNet on CIFAR-100+ with the two dropout variants in Figure 10. The left panel indicates that the regularization effect of the drop-neuron training is rather limited, which is mainly because the channel instead of the neuron is the more suited structural level for the regularization of the convolutional transformation. Compared with drop-neuron, drop-channel regularizes the model effectively and thus achieves significantly better performance. With drop-channel, the test error decreases faster, and the training is more stable, especially before the first learning rate drop at epoch 150. Furthermore, DenseNet regularized by drop-channel learns with higher training loss while with much lower test error, indicating that drop-channel prevents overfitting effectively.

## 5 CONCLUSION

In this paper, we formulated and examined the three structural levels of dropout training with a unified convolutional transformation framework, including drop-neuron,

drop-channel drop-path. We attribute the failure of standard dropout to the incorrect placement in the convolutional building block, which incurs great training instability. Through detailed discussion and analysis, we propose general convolutional building blocks supporting different structural levels of dropouts and a more effective variant drop-conv2d, which are better in line with the convolutional transformation for CNNs and incurs negligible additional training costs.

Extensive analysis and experiments have shown that firstly, all these dropout variants are effective in improving the performance of convolutional neural networks by a noticeable margin. Further, among these dropout methods, drop-neuron and drop-channel are widely applicable to existing CNNs, while drop-path and particularly drop-layer are highly dependent on the CNN architecture. In terms of effectiveness, drop-channel generally outperforms other dropout variants. This is largely due to the characteristic of the convolution transformation of CNNs, where the channel instead of other structural components is the most fundamental units participating in the operation. Therefore, drop-channel can better harness the benefits of both regularization and model ensemble. We further note that drop-channel could be more effective with Group Normalization. Further, drop-neuron and drop-channel can be integrated with higher levels of dropout variants, e.g., drop-path, which can further stabilize the training process. On the other hand, drop-neuron outperforms drop-channel in the network trained without data augmentation.

With the proposed building blocks designed for dropout training mechanisms, we can achieve noticeable improvement over state-of-the-art CNNs on CIFAR-10/100, SVHN and ImageNet datasets. Given the generality and flexibility, these dropout training mechanisms would be useful for improving the training of a wide range of deep CNNs.

## REFERENCES

- [1] P. Baldi, P. J. Sadowski, Understanding dropout, *Advances in Neural Information Processing Systems*, pages 2814–2822, 2013.
- [2] S. Cai, G. Chen, B. C. Ooi, J. Gao, Model slicing for supporting complex analytics with elastic inference cost and resource constraints, *PVLDB*, 13(2):86–99, 2019.
- [3] J. Dai, M. Zhang, G. Chen, J. Fan, K. Y. Ngiam, B. C. Ooi, Fine-grained concept linking using neural networks in healthcare, *Proceedings of the 2018 International Conference on Management of Data*, pages 51–66. ACM, 2018.
- [4] T. Devries, G. W. Taylor, Improved regularization of convolutional neural networks with cutout, *CoRR*, abs/1708.04552, 2017.
- [5] Y. Gal, Z. Ghahramani, Dropout as a bayesian approximation: Representing model uncertainty in deep learning, *international conference on machine learning*, pages 1050–1059, 2016.
- [6] G. Ghiasi, T. Lin, Q. V. Le, Dropblock: A regularization method for convolutional networks, *Advances in Neural Information Processing Systems 2018, NeurIPS*, pages 10750–10760, 2018.
- [7] K. He, X. Zhang, S. Ren, J. Sun, Deep residual learning for image recognition, *Proceedings of the IEEE conference on computer vision and pattern recognition*, pages 770–778, 2016.
- [8] K. He, X. Zhang, S. Ren, J. Sun, Identity mappings in deep residual networks, *European Conference on Computer Vision*, pages 630–645. Springer, 2016.
- [9] D. Hendrycks, K. Gimpel, Adjusting for dropout variance in batch normalization and weight initialization, *arXiv preprint arXiv:1607.02488*, 2016.
- [10] G. E. Hinton, N. Srivastava, A. Krizhevsky, I. Sutskever, R. R. Salakhutdinov, Improving neural networks by preventing co-adaptation of feature detectors, *arXiv preprint arXiv:1207.0580*, 2012.
- [11] S. Hochreiter, J. Schmidhuber, Long short-term memory, *Neural computation*, 9(8):1735–1780, 1997.
- [12] A. G. Howard, M. Zhu, B. Chen, D. Kalenichenko, W. Wang, T. Weyand, M. Andreetto, H. Adam, Mobilenets: Efficient convolutional neural networks for mobile vision applications, *arXiv preprint arXiv:1704.04861*, 2017.
- [13] J. Hu, L. Shen, G. Sun, Squeeze-and-excitation networks, *2018 IEEE Conference on Computer Vision and Pattern Recognition, CVPR*, pages 7132–7141, 2018.
- [14] G. Huang, Z. Liu, L. Van Der Maaten, K. Q. Weinberger, Densely connected convolutional networks, *Proceedings of the IEEE conference on computer vision and pattern recognition*, 2017.
- [15] G. Huang, Y. Sun, Z. Liu, D. Sedra, K. Q. Weinberger, Deep networks with stochastic depth, *European Conference on Computer Vision*, pages 646–661, 2016.
- [16] S. Ioffe, C. Szegedy, Batch normalization: Accelerating deep network training by reducing internal covariate shift, *International Conference on Machine Learning*, pages 448–456, 2015.
- [17] D. P. Kingma, T. Salimans, M. Welling, Variational dropout and the local reparameterization trick, *Advances in Neural Information Processing Systems*, pages 2575–2583, 2015.
- [18] A. Krizhevsky, G. Hinton, Learning multiple layers of features from tiny images, *Tech Report*, 2009.
- [19] A. Krizhevsky, I. Sutskever, G. E. Hinton, Imagenet classification with deep convolutional neural networks, *Advances in neural information processing systems*, pages 1097–1105, 2012.
- [20] G. Larsson, M. Maire, G. Shakhnarovich, Fractalnet: Ultra-deep neural networks without residuals, *5th International Conference on Learning Representations, ICLR*, 2017.
- [21] X. Li, S. Chen, X. Hu, J. Yang, Understanding the disharmony between dropout and batch normalization by variance shift, *Proceedings of the IEEE Conference on Computer Vision and Pattern Recognition*, pages 2682–2690, 2019.
- [22] M. Lin, Q. Chen, S. Yan, Network in network, *2nd International Conference on Learning Representations, ICLR*, 2014.
- [23] H. Liu, K. Simonyan, Y. Yang, DARTS: differentiable architecture search, *7th International Conference on Learning Representations, ICLR*, 2019.
- [24] Y. Netzer, T. Wang, A. Coates, A. Bissacco, B. Wu, A. Y. Ng, Reading digits in natural images with unsupervised feature learning, *NIPS workshop on deep learning and unsupervised feature learning*, volume 2011, page 5, 2011.
- [25] Y. Shu, W. Wang, S. Cai, Understanding architectures learnt by cell-based neural architecture search, *8rd International Conference on Learning Representations, ICLR*, 2020.
- [26] K. Simonyan, A. Zisserman, Very deep convolutional networks for large-scale image recognition, Y. Bengio, Y. LeCun, editors, *3rd International Conference on Learning Representations, ICLR*, 2015.
- [27] N. Srivastava, G. E. Hinton, A. Krizhevsky, I. Sutskever, R. Salakhutdinov, Dropout: a simple way to prevent neural networks from overfitting., *Journal of machine learning research*, 15(1):1929–1958, 2014.
- [28] C. Szegedy, S. Ioffe, V. Vanhoucke, A. A. Alemi, Inception-v4, inception-resnet and the impact of residual connections on learning., *AAAI*, pages 4278–4284, 2017.
- [29] C. Szegedy, W. Liu, Y. Jia, P. Sermanet, S. Reed, D. Anguelov, D. Erhan, V. Vanhoucke, A. Rabinovich, Going deeper with convolutions, *Proceedings of the IEEE conference on computer vision and pattern recognition*, pages 1–9, 2015.
- [30] J. Tompson, R. Goroshin, A. Jain, Y. LeCun, C. Bregler, Efficient object localization using convolutional networks, *Proceedings of the IEEE Conference on Computer Vision and Pattern Recognition*, pages 648–656, 2015.
- [31] A. Veit, M. J. Wilber, S. Belongie, Residual networks behave like ensembles of relatively shallow networks, *Advances in Neural Information Processing Systems*, pages 550–558, 2016.
- [32] S. Wager, S. Wang, P. S. Liang, Dropout training as adaptive regularization, *Advances in neural information processing systems*, pages 351–359, 2013.
- [33] L. Wan, M. Zeiler, S. Zhang, Y. Le Cun, R. Fergus, Regularization of neural networks using dropconnect, *International Conference on Machine Learning*, pages 1058–1066, 2013.
- [34] Y. Wu, K. He, Group normalization, *Proceedings of the European Conference on Computer Vision (ECCV)*, pages 3–19, 2018.
- [35] S. Xie, R. Girshick, P. Dollár, Z. Tu, K. He, Aggregated residual transformations for deep neural networks, *2017 IEEE Conference on Computer Vision and Pattern Recognition (CVPR)*, 2017.
- [36] Y. Yamada, M. Iwamura, K. Kise, Shakedown regularization, *6th International Conference on Learning Representations, ICLR*, 2018.
- [37] S. Zagoruyko, N. Komodakis, Wide residual networks, *Proceedings of the British Machine Vision Conference 2016, BMVC*, 2016.
- [38] M. D. Zeiler, R. Fergus, Visualizing and understanding convolutional networks, *European conference on computer vision*, pages 818–833. Springer, 2014.
- [39] K. Zheng, S. Cai, H. R. Chua, W. Wang, K. Y. Ngiam, B. C. Ooi, Tracer: A framework for facilitating accurate and interpretable analytics for high stakes applications, *Proceedings of the 2020 International Conference on Management of Data, SIGMOD*, 2020.
- [40] B. Zoph, Q. V. Le, Neural architecture search with reinforcement learning, *5th International Conference on Learning Representations, ICLR*, 2017.